ISBN: 978-3-95450-208-0 doi:10.18429/JACoW-IPAC2019-TUPTS104

SPATIO-TEMPORAL SHAPING OF THE PHOTOCATHODE LASER PULSE FOR LOW-EMITTANCE SHAPED ELECTRON BUNCHES*

T. Xu[1†], C. Jing[2], A. Kanareykin[2], P. Piot[1,3], J. G. Power[4],
[1]Northern Illinois University, DeKalb, IL 60115, USA
[2]Euclid Techlabs LLC., Bolingbrook, IL 60516, USA
[3]Fermi National Accelerator Laboratory, Batavia, IL 60510, USA
[4]Argonne National Laboratory, Lemont, IL 60439, USA

Abstract

Photocathode laser shaping techniques to generate temporally shaped electron bunches are appealing owing to their simplicity. Such a technique is being considered to form shaped electron bunches to enhance the transformer ratio in beam-driven accelerators. At low energy (i.e. during the emission process) the transverse and longitudinal space charge effects are coupled so that attaining a low beam transverse emittance require the laser to be spatiotemporal shaped. In this paper, we explore the generation of a linearly-ramped bunch with optimized transverse emittance by temporally and radially shaping the laser pulse to provide an adequate initial distribution. We discuss the possible implementation of the optical shaping technique and describe a planned experiment.

INTRODUCTION

Femtosecond laser shaping technique has demonstrated to be a useful experimental tool by providing the capability to precisely control ultrafast laser waveforms [1]. Arbitrarily shaped laser pulses have found applications in many fields including spectroscopy, nonlinear optics, and biological imaging [2]. For the physics of photoinjectors, shaping of drive laser pulses at photocathode enables the formation of optimized electron beam distribution in support of various applications. In particular, a longitudinally shaped electron beam is critical to the realization of efficient beam-driven acceleration. In this acceleration scheme, a drive particle bunch passes through a high impedance structure and excites a wakefield. With proper configuration, this wakefield can be used to accelerate a trailing low-charge "witness" bunch. It has been recognized that drive bunch with a tailored current profile (e.g. linearly-ramped, or "doorstep" distributions) can significantly improve the transformer ratio in beam-drive accelerator compared with symmetric (e.g. Gaussian) current profiles [3].

Over the last two decades, various beam-shaping techniques have been proposed and investigated. These include. e.g., transverse-to-longitudinal phase-space emittance exchange [4], multi-frequency linacs [5], interaction with wakefields [6]. Among those longitudinal shaping schemes, photocathode-laser shaping yields ample flexibility and great simplicity. It directly manipulates the distribution of electron bunch at photocathode while requiring no extra modification of the accelerator beamline. However, in the case of a high-charge bunch or peak-field on the photocathode, the electron bunch will be significantly influenced by space-charge effects which, in turn, will influence the shaping process and possibly degrade the transverse beam emittances.

In this paper, we discuss a proof-of-principle experiment being planned at the Argonne Wakefield Accelerator (AWA) aimed at investigating spatiotemporal shaping of the photocathode laser pulse to produce bunch with parameters consistent with beam-driven acceleration [7]. We especially show, through optimization of the laser-pulse distribution and beamline parameters that a low-emittance, high-charge, longitudinally-shaped electron bunch can be generated and preserved during acceleration.

OPTIMIZED BUNCH FROM A SPATIOTEMPORALLY-SHAPED LASER PULSE

In the absence of collective and nonlinear effects, the distribution of an electron bunch photoemitted from photocathode mirrors the laser pulse distribution. During the acceleration in RF gun, the bunch is susceptible to nonlinear distortions imparted via space charge or due to nonlinearities associated with the RF fields. In the present work, we consider the generation of a low-emittance electron bunch with a linearly-ramped current profile (where the head of the bunch has a lower charge than its tail). In order to produce the desired final current distribution and suppress emittance growth, we extend our previous work [8] to allow for the optimization of the laser-pulse spatiotemporal distribution (t, r).

Several possible parameterizations were investigated and here we study the case where the laser temporal intensity follows the distribution,

$$f\left(\frac{t}{T_{\max}}\right) = a\left(1 - \frac{t}{T_{\max}}\right)^{a-1}, 1 < a < 2. \quad (1)$$

Given the temporal probability density function (PDF) $f(t)$, the radial coordinates is taken to satisfy

$$\left(\frac{r}{R_{\max}}\right)^b + \left(\frac{t}{T_{\max}}\right)^c \leq 1 \quad (2)$$

* This work was supported by the US Department of Energy (DOE) contracts No. DE-SC0018656 with NIU and No. DE-AC02-06CH11357 with ANL.
† xu@niu.edu

ISBN: 978-3-95450-208-0 doi:10.18429/JACoW-IPAC2019-TUPTS104

where T_{max} is the full laser-pulse duration and R_{max} is the maximum laser spot radius. The exponents a, b, and c, along with the constants T_{max} and R_{max}, are free variables determined in optimization. Practically, we use a Monte-Carlo technique to generate a macroparticle distribution with PDF described by the two previous equations. The distribution is generated in the (ζ, r) space (where $\zeta \equiv \beta ct$ is the longitudinal coordinates in the bunch frame and βc the particle velocity at emission).

The beam-dynamics simulation are performed with with IMPACT-T, a particle-in-cell beam-dynamics program that includes 3D space-charge effects [9]. Since both current distribution and emittance are of interest in our case, we implemented a multi-objective optimization with DEAP evolutionary computation framework.

To quantitatively compare the final simulated current profile with the target distribution, we use the Wasserstein distance [10] customarily used in statistics. Suppose $P(z)$ is the longitudinal distribution of simulated macro-particles with $z \in [0, 1]$ being the normalized longitudinal coordinate. The PDF of distribution $P(z)$ can be computed using a kernel density estimation technique. Then for a given target distribution $Q(z)$, we calculate their 1st Wasserstein distance as,

$$W_1(P, Q) = \int_{-\infty}^{+\infty} |p(z) - q(z)| dz \qquad (3)$$

where $p(z)$ and $q(z)$ are the normalized cumulative distribution functions (CDF) respectively obtained from the PDFs $P(z)$ and $Q(z)$.

Figure 1 exemplifies the 1st Wasserstein distance comparing the PDF and CDF associated with a Monte-Carlos-sampled skewed-Gaussian with a power-law target distribution (power function). The shaded area in Fig 1(right) represents the integrand of Eq. 3. Aside from the parameters related to laser pulse distribution, the optimizer was also allowed to vary gun phase, solenoid strengths and linac phases.

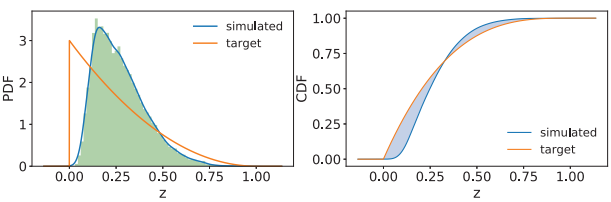

Figure 1: PDFs (left) of a simulated skewed Gaussian distribution (blue shaded trace) and power-law target distribution (orange trace) along with associated CDFs (right).

We performed beam-dynamics simulations using the AWA drive-beam photoinjector diagrammed in Fig. 2. The beamline incorporates a 1+1/2 L-band (1.3 GHz) RF gun followed by six 7-cell cavities. The RF-gun cavity is surrounded by three solenoidal lenses and includes a Cs_2Te photocathode which is impinged by an ultraviolet laser pulse obtained via frequency tripling of an amplified infrared laser. In our simulation two of the linac cavities (C4 and C6) were turned off to mimic one of the standard-operating configurations. The resulting beam parameters obtained downstream

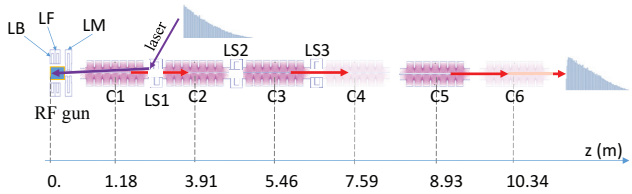

Figure 2: Layout of the AWA drive-beam photoinjector beamline. The C*i* labels refer to accelerating cavity [the shaded cavities (C4 and C6) were turned off in our simulations]. L*i* are solenoidal lenses.

of the linac is summarized in Table 1 together with some of the associated accelerator settings. Snapshots of the transverse and longitudinal phase space at different locations along the beamline appear in Figure 3. Compared to our

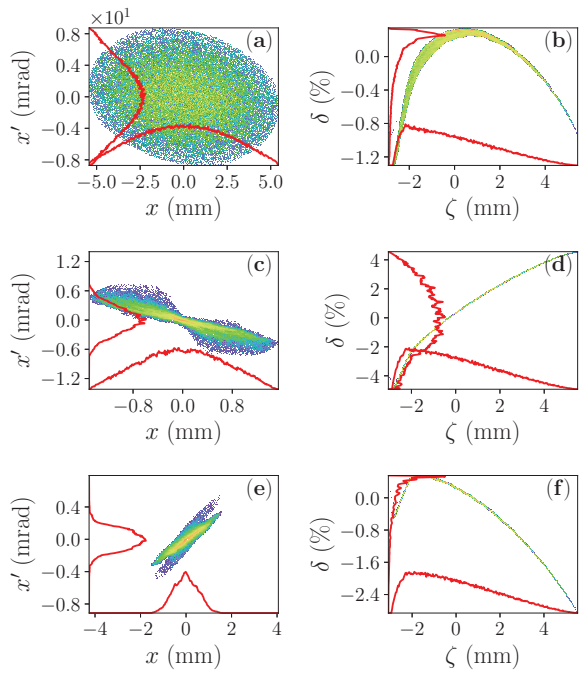

Figure 3: Transverse (a, c, e) and longitudinal (b, d, f) phase space snapshots downstream of the RF gun (a,b), cavity C1 (c,d), and cavity C6 (e,f). The head of the bunch corresponds to $\zeta > 0$.

previous work [8] which only considered temporal shaping, we find that the spatiotemporal shaping improves the beam emittance while maintaining similar performances to shape the final current profile. One limitation associated with the temporal profile discussed in [8] stems from large variation in charge density $Q/[\Delta\zeta \times \pi r^2(\zeta)]$ between longitudinal slices with length $\Delta\zeta$ (leading the bunch tail to have a much higher density than the head). Such imbalance exacerbates distortions originating from space charge effects (and eventually from additional collective effects in the subsequent

ISBN: 978-3-95450-208-0 doi:10.18429/JACoW-IPAC2019-TUPTS104

beamline). It especially results in some particles located in the bunch head to acquire large orbit due to over-focusing. In the present spatiotemporal optimization such a deleterious effect is minimized as illustrated in Fig. 4(right).

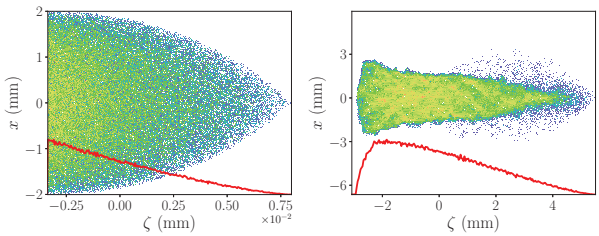

Figure 4: Initial (left) and final (right) (ζ, x) distribution obtained after optimization. The initial distribution is simulated at the cathode location with a 0.55-eV kinetic energy.

Table 1: Accelerator Settings and Simulated Beam Parameters Downstream of C6 Associated with One Set of Optimized Parameters

Parameter	Value	Units
Number of macroparticles	200,000	–
Bunch charge	3	nC
Emission time	26	ps
Laser spot radius	2	mm
RF gun peak E field	35	MV/m
laser launch phase	50	deg
Final beam energy	43	MeV
Final transverse emittance	1.5	μm-rad
Final RMS bunch length	1.8	mm

LASER SHAPER

The generation of optical pulses we ramped temporal distribution was recently demonstrated [11]. An upgraded version of the AWA photocathode-laser system will be used to explore spatiotemporal laser shaping starting from the work of Ref. [11]. In brief, the infrared (IR) pulses are produced in a commercial oscillator locked to the AWA master oscillator. The sub-100-fs pulses with central wavelength $\lambda_0 = 785$ nm and $\Delta\lambda \simeq 35$-nm bandwidth is filtered and amplified in a chirped-pulse amplifier before being frequency tripled to reach the necessary photon energy for photoemission from a Cs_2Te cathode (corresponding to $\lambda = 265$ nm). The pulse shaping will be performed in the IR path owing to the simpler implementation. Its performance will be to be optimized to form the required ultraviolet (UV) shapes needed to produce electron bunches with tailored temporal distributions. Among the various pulse-shaping methods available [1] and given the successful resulted presented in [11], we selected a frequency-domain method employing a digital programmable mask. A first version of the shaper will consist of a folded configuration consisting of a grating that introduces the needed dispersion followed by a collimating lens and reflective nematic liquid crystal spatial-slight modulator (SLM). In a later iteration, the SLM (which consists of a 1-d array of pixelized stripes) will be replaced by a digital micro-mirror device (DMD) (2-d pixel array) so to allow for spatiotemporal shaping along one direction. The system requires the incoming laser pulse to be chirped so to introduce a linear correlation between rate and time.

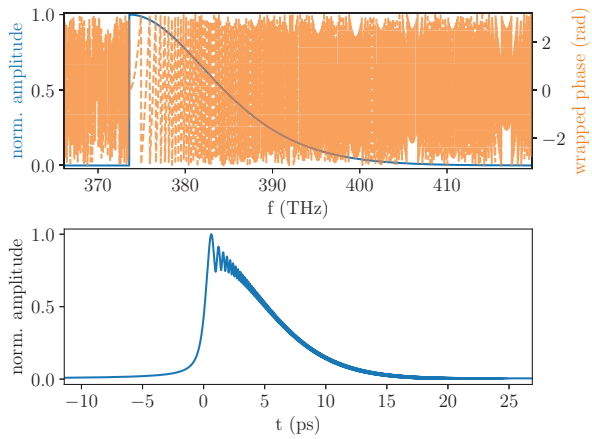

Figure 5: Spectrum (upper plot) associated with a dispersed laser pulse with clipped frequencies $f < f_0$ and associated temporal distribution (lower plot) after the shaper. The blue and orange traces in the upper plot correspond respectively to the spectral amplitude and wrapped phase.

A simple time-frequency program was developed based on the PYNLO [12] module to allow for the exploration of temporal shaping. The extension to fully 3D simulation will be performed with the SRW package [13]. An example of simulation produced by chirping the initial pulse to introduce a group-delay dispersion (GDD) $D_2 = 0.09$ ps^2 and clipping the lower part of the spectrum $< f_0 \equiv 2\pi c/\lambda_0$ appear in Fig.5. The produced laser pulse display some high-frequency oscillation due to the limited bandwidth (taken to be 15 nm here) as observed experimentally [11]. The impact of such oscillations on the beam dynamics remains to be analyzed.

CONCLUSION

The beam dynamics associated with the generation of electron bunches with shaped current profiles is intricately related to the photocathode-laser shape. In this paper we demonstrated that with proper optimization a $\sim$ 40-MeV 3-nC electron bunch with linearly-ramped current profile could be achieved with low tranverse emittances. A critical aspect is to control the spatiotemporal shape of the photocathode laser. Producing the required tailored laser pulse is challenging and an experiment is in preparation at the AWA facility. The required 3D optical simulations are currently being developed.

ISBN: 978-3-95450-208-0 doi:10.18429/JACoW-IPAC2019-TUPTS104

REFERENCES

[1] A. M. Weiner, "Femtosecond pulse shaping using spatial light modulators," *Rev. Sci. Instrum.*, vol. 71, no. 5, pp. 1929–1960, 2000.

[2] A. Monmayrant, S. Weber, and B. Chatel, "A newcomer's guide to ultrashort pulse shaping and characterization," *Journal of Physics B: Atomic, Molecular and Optical Physics*, vol. 43, no. 10, p. 103001, 2010.

[3] K. L. Bane, P. Chen, and P. B. Wilson, "On collinear wake field acceleration," *Proc. of the 1985 Part. Accel. Conf. (PAC1985): Accelerator Engineering and Technology Vancouver, BC May 13-16, 1985*, vol. 32, pp. 3524–3526, 1985.

[4] G. Ha, M. H. Cho, W. Namkung, J. G. Power, D. S. Doran, E. E. Wisniewski, M. Conde, W. Gai, W. Liu, C. Whiteford, Q. Gao, K.-J. Kim, A. Zholents, Y.-E. Sun, C. Jing, and P. Piot, "Precision control of the electron longitudinal bunch shape using an emittance-exchange beam line," *Phys. Rev. Lett.*, vol. 118, p. 104801, Mar 2017.

[5] P. Piot, C. Behrens, C. Gerth, M. Dohlus, F. Lemery, D. Mihalcea, P. Stoltz, and M. Vogt, "Generation and Characterization of Electron Bunches with Ramped Current Profiles in a Dual-Frequency Superconducting Linear Accelerator," *Phys. Rev. Lett.*, vol. 108, p. 034801, Jan. 2012.

[6] G. Andonian, S. Barber, F. H. O'Shea, M. Fedurin, K. Kusche, C. Swinson, and J. B. Rosenzweig, "Generation of ramped current profiles in relativistic electron beams using wakefields in dielectric structures," *Phys. Rev. Lett.*, vol. 118, p. 054802, Feb 2017.

[7] F. Lemery and P. Piot, "Tailored electron bunches with smooth current profiles for enhanced transformer ratios in beam-driven acceleration," *Phys. Rev. Spec. Top.–Accel. Beams*, vol. 18, no. 8, p. 081301, 2015.

[8] T. Xu, C. Jing, A. Kanareykin, P. Piot, and J. Power, "Optimized Electron Bunch Current Distribution from a Radiofrequency Photo-Emission Source," in *2018 IEEE Advanced Accelerator Concepts Workshop (AAC)*, (Breckenridge, CO, USA), pp. 1–5, IEEE, Aug. 2018.

[9] J. Qiang, S. Lidia, R. D. Ryne, and C. Limborg-Deprey, "Three-dimensional quasistatic model for high brightness beam dynamics simulation," *Phys. Rev. ST Accel. Beams*, vol. 9, p. 044204, Apr 2006.

[10] A. Ramdas, N. Trillos, and M. Cuturi, "On wasserstein two-sample testing and related families of nonparametric tests," *Entropy*, vol. 19, no. 2, p. 47, 2017.

[11] I. Kuzmin, S. Mironov, E. Gacheva, V. Zelenogorsky, A. Potemkin, E. Khazanov, A. Kanareykin, S. Antipov, M. Krasilnikov, G. L. oisch, and F. Stephan, "Shaping triangular picosecond laser pulses for electron photoin jectors," *Laser Physics Letters*, vol. 16, p. 015001, nov 2018.

[12] J. Hult, "A fourth-order runge–kutta in the interaction picture method for simulating supercontinuum generation in optical fibers," *J. Lightwave Technol.*, vol. 25, pp. 3770–3775, Dec 2007.

[13] O. Chubar, A. Fluerasu, L. Berman, K. Kaznatcheev, and L. Wiegart, "Wavefront propagation simulations for beamlines and experiments with "synchrotron radiation workshop"," *Journal of Physics: Conference Series*, vol. 425, p. 162001, mar 2013.